CNRS - Université Pierre et Marie Curie - Université Versailles-Saint-Quentin
CEA - ORSTOM - Ecole Normale Supérieure - Ecole Polytechnique

Institut Pierre Simon Laplace
des Sciences de l'Environnement Global

Notes du Pôle de Modélisation

Transient properties of atmospheric circulation in two reanalysis datasets

Z.X. Li (1) and A.F. Carril (2)

(1) Laboratoire de Météorologie Dynamique du CNRS
(2) Centro de Investigaciones del Mar y la Atmósfera, Buenos Aires

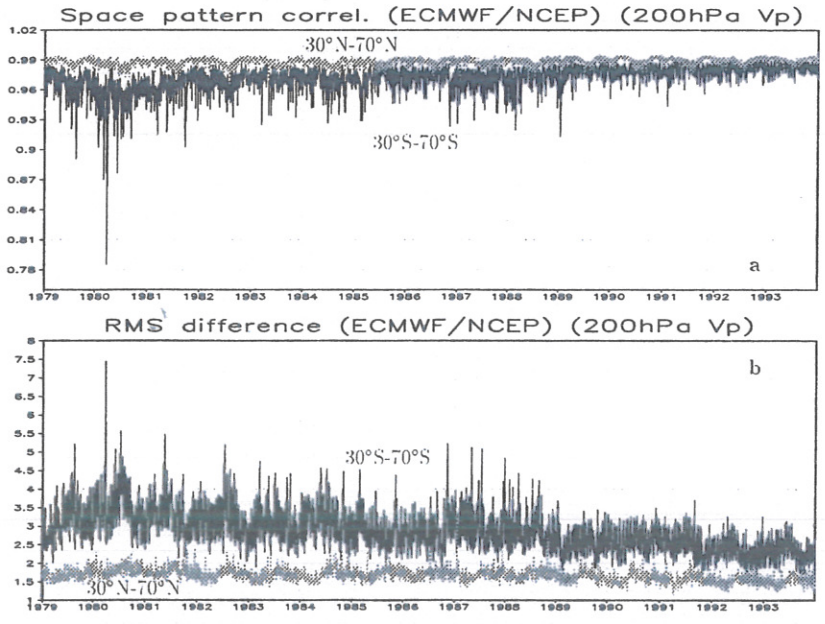

Novembre 1998 **Note n° 10**

I P S L

CNRS - Université Pierre et Marie Curie - Université Versailles-Saint-Quentin
CEA -CNES - ORSTOM - Ecole Normale Supérieure - Ecole Polytechnique

Institut Pierre Simon Laplace
des Sciences de l'Environnement Global

CETP - LMD - LODYC - LPCM - LSCE - SA

Université Pierre-et-Marie-Curie
B 102 - T15-E5 - 4, Place Jussieu
75252 Paris Cedex 05 (France)
Tél : (33) 01 44 27 39 83
Fax : (33) 01 44 27 37 76

Université Versailles-Saint-Quentin
College Vauban, 47 Boulevard Vauban
78047 Guyancourt Cedex (France)
Tél : (33) 01 39 25 58 17
Fax : (33) 01 39 25 58 22

Transient properties of atmospheric circulation in two reanalysis datasets

Z.X. Li (1) and A.F. Carril (2)

(1) Laboratoire de Météorologie Dynamique du CNRS
(2) Centro de Investigaciones del Mar y la Atmósfera, Buenos Aires

Les caractéristiques transitoire de la circulation générale atmosphérique sont étudiées à travers deux jeux de données fournis respectivement par ECMWF et NCEP. La période commune de ces deux jeux de données est de 1979 à 1993. D'une manière générale, la comparaison donne un très bon accord pour l'hémisphère du nord. En revanche, pour l'hémisphère du sud où le réseau d'observation est moins dense, beaucoup de différences existent. Les transports transitoires du moment angulaire et du flux de chaleur sont de 20% plus faibles dans NCEP que dans ECMWF. Ces différences sont principalement dues au fait que les événements transitoires dans NCEP ont une plus faible amplitude par rapport à ceux dans ECMWF. Mais leur évolution temporelle et leur structure spatiale ont un bon accord entre ces deux jeux de données.

Novembre 1998
Note n° 10

Directeur de publication : Gérard Mégie, Directeur de l'IPSL
Demande de n° ISSN en cours

Z.X. Li, A.F. Carril

Transient properties of atmospheric circulation in two reanalysis datasets

---

Z.X. Li

Laboratoire de Météorologie Dynamique du CNRS, casier 99, Université P. et M. Curie, 4 Place Jussieu, 75252 Paris cedex 05, France ; e-mail : li@lmd.jussieu.fr

A.F. Carril

Centro de Investigaciones del Mar y la Atmósfera, PAB II, 2o piso, Ciudad Universitaria, 1428 Buenos Aires, Argentina ; e-mail : carril@at1.fcen.uba.ar

Abstract. The transient behavior of the atmospheric circulation is examined in two reanalysis datasets provided respectively by NCEP (National Centers for Environmental Prediction, NOAA) and ECMWF (European Center for Medium-range Weather Forecasts). The time period for both datasets covers 1979-1993. The agreement between the two reanalyses is, in general, good in the Northern Hemisphere. But in the Southern Hemisphere, considerable discrepancies exist over the data-poor regions. The transient kinetic energy, the meridional transient flux of heat and angular momentum are about 20% smaller in NCEP than in ECMWF. These differences are mainly due to the fact that transient events have smaller amplitude in NCEP than in ECMWF. However their time evolution and space pattern agree well between the two datasets.

1 Introduction

The transient behavior of the atmospheric circulation is an important component of the general circulation. The studies on the occurrence, amplitude and time evolution of transient waves contribute directly to the understanding and forecasting of mid-latitude storm tracks and blockings. Recently, in order to obtain a complete and more consistent dataset of the atmosphere's structure, several weather service centers have reanalyzed the past observational data by using the most advanced data assimilation systems and the state-of-the-art numerical forecast models. At present, the most important reanalyses available for the scientific community are those realized at ECMWF (European Center for Medium-range Weather Forecasts), NOAA/NCEP (National Centers for Environmental Prediction) and NASA/DAO (Data Assimilation Office).

The advantages of reanalyses are their consistency and homogeneity in time. Compared to the daily operational analyses, the reanalyses utilize more historical observations and can reach a more accurate analysis of the atmospheric circulations and a more accurate representation for data-poor regions. There are, however, limitations to the accuracy of the reanalyzed datasets. Systematic errors in numerical models can cause errors in the assimilation of observed data and large biases in data-poor regions. The atmospheric evolution as depicted by the different reanalysis systems can be expected to show discrepancies.

The purpose of this paper is to document and compare the transient behaviors of the atmospheric circulation between the reanalysis of ECMWF and that of NCEP. Lack of independent information will not permit us to judge on the quality of the two products, but the comparison can serve as a measure of the uncertainty. The plan of the paper is as follows. We

present our data processing method in Section 2. Section 3 gives the results and conclusions follow in Section 4.

2 Data and analysis method

The NCEP reanalysis system utilizes a 28-level global spectral model at the resolution T62. Detailed descriptions of the model, the analysis procedures, and the input data are given in Kalnay et al. (1996). The data used in this paper are at the resolution 2.5° for both latitude and longitude. They are daily averaged temperature T, zonal wind u and meridional wind v for the period 1979 to 1993 and at twelve standard pressure levels : 1000, 925, 850, 700, 600, 500, 400, 300, 250, 200, 150, and 100 hPa. The ECMWF reanalysis (ERA) is produced from a T106 data assimilation system. The model has 31 vertical hybrid levels. The original data are available at the full resolution of 1.125° and 4 times per day. More information about the ERA system and data sources can be found in Gibson et al. (1996). In order to overcome the comparison difficulties related to grid difference, we first transform the ECMWF's data into the grid of NCEP, and perform daily averaging. The time period is the same as for NCEP (1979-1993). The 12 vertical pressure levels are also the same. The two datasets have thus same time period, same spatial and temporal resolution before the analysis processing is applied.

To determine the transient quantity, we have to fix the mean term. We use the calendar month as our basic time unit, that is, we calculate the mean and covariance terms for respectively the twelve calendar months. These quantities are : $\overline{u}$, $\overline{v}$, $\overline{T}$, $\overline{uu}$, $\overline{vv}$, $\overline{TT}$, $\overline{vu}$ and $\overline{vT}$, where a bar denotes a time average. The transient quantities can be then deduced from the residual of the

mean term and the covariance term (Peixoto and Oort 1992). For example, the meridional transient zonal angular momentum flux can be obtained by :

$$\overline{v'u'} = \overline{vu} - \bar{v} \cdot \bar{u}$$

where a prime denotes a departure from the time average. The seasonal quantities showed throughout this paper are the 3-month average of the above monthly quantities. In this way, we can remove the contribution from variations longer than a month, including the annual cycle and interannual variations.

3 Results

3.1 Mean field

Before discussing the transient quantities, we examine briefly some mean climatology fields. Figure 1 shows the difference (ECMWF minus NCEP) of the annual and zonal mean temperature. The most remarkable difference is that the tropopause in ECMWF is colder and the amplitude can reach -2.5°C in the Tropics. This seems related to the tropopause shift between the two datasets. Utilization of different parameterization schemes (especially convection and radiation) is certainly responsable for this tropopause shift. Large discrepancies are also observed for high latitudes of the Southern Hemisphere. Antarctica is much colder in NCEP than in ECMWF, especially in winter season (the same tendency is also observed over Greenland in Northern Hemisphere winter). The difference is generally small in the Northern Hemisphere, especially between 30°N and 70°N where data sources are more abundant.

For the mean zonal wind (figure not shown), the agreement between the two datasets is very good in the Northern Hemisphere. In the Tropics, the easterlies are slightly stronger in NCEP than in ECMWF. In the Southern Hemisphere, the sub-tropical jet is 1 to 2 m s^{-1} stronger in ECMWF than in NCEP. The sub-polar jet (visible mainly in austral winter) is also stronger in ECMWF than in NCEP.

3.2 Transient eddy kinetic energy

The transient kinetic energy, K_e, defined as $\left(\overline{u'^2} + \overline{v'^2}\right)\Big/2$, is an overall measure of the amplitude of transient activities. Figure 2 shows the vertical structure of the zonal-mean transient kinetic energy in the two datasets for both December-January-February (DJF) and June-July-August (JJA) seasons. In the Northern Hemisphere, the two datasets are very close to each other. In the Southern Hemisphere, however, the transient kinetic energy is considerably smaller in NCEP than in ECMWF. This is true for both DJF and JJA.

Figure 3a shows the 200-hPa annual-mean transient kinetic energy in NCEP. The strong-value regions are over North Pacific, North Atlantic and mid-latitudes of the Southern Hemisphere. They correspond to large transient activities of the atmosphere. Small values are found in the Tropics and polar regions. The panels b and c of Fig. 3 show respectively the algebraic difference and RMS (root-mean-square) difference between ECMWF and NCEP. In the Northern Hemisphere, the agreement between the two datasets is in general good. However, ECMWF is about 5 m^2 s^{-2} smaller than NCEP, and the RMS difference can reach 50 even 60 m^2 s^{-2} over North Atlantic and North Pacific. For equatorial Pacific, ECMWF is 5 m^2 s^{-2} smaller than NCEP in the eastern part, but larger in the western part. In the Southern Hemisphere, as indicated

before, the transient kinetic energy is systematically smaller in NCEP than in ECMWF, except over Australia and New Zealand where the observation network is relatively dense. The difference over Austral Oceans can reach 50 $m^2 s^{-2}$ and the RMS difference 100 $m^2 s^{-2}$. It is clear that the lack of reliable observation over these regions is the principal cause of this large discrepancy.

An interesting contrast (negative and positive signs) can be observed in Fig. 3b between the Northern and Southern Hemispheres, or between data-rich and data-poor regions. This is probablly related to the difference in resolution of models and the treatment of dissipation processes. The poor resolution of NCEP model makes it less suitable to resolve the baroclinic waves in the Southern Hemisphere so its transient kinetic energy is deficient. At the same time, the dissipation could be tuned to a very low level to compensate the poor resolution, and this might explain why the transient kinetic energy in NCEP is excessive compared to ECMWF for the data-rich regions.

3.3 Meridional transient flux of angular momentum and sensible heat

These quantities are good indicators of baroclinic wave growth (Simmons and Hoskins 1978) and of dynamical interaction between transient eddies and mean flow (Edmon et al. 1980 ; Hoskins et al. 1983). They contribute to the global balances of angular momentum and energy. Especially they determine the way in which these balances are realized. Figure 4 displays the latitude-pressure diagram of the meridional transient flux of zonal angular momentum, $\overline{v'u'}$. The maximum transport occurs between 200 and 300 hPa. The agreement between NCEP and ECMWF is in general good in the Northern Hemisphere, although the maximum center over 30°N is slightly stronger in NCEP than in ECMWF. But in the Southern Hemisphere, the

difference is remarkable : around 30°S (in JJA) and 40°S (in DJF), NCEP is 20% smaller than ECMWF.

Figure 5 displays the meridional transient flux of sensible heat, $\overline{v'T'}$. For the mid-latitudes of both the hemispheres, we can observe two maximum centers, one is at low level (850 hPa), another is at high level (200 hPa). The direction of the transport is polarward. Note that in the Tropics between 30°S and 30°N, we can observe small equatorward heat transport by the transient eddies in the middle levels of the atmosphere. We now compare the two datasets. The agreement is quite good in the Northern Hemisphere for both seasons. Large discrepancies can be found in the Southern Hemisphere. For low levels, the NCEP's transport is about 15% smaller than that of ECMWF. The value of the active center at 65°S and 930 hPa is stronger in NCEP, but a careful verification reveals that this is due to excessive values in the region of East Antarctica (Wilkes land), where extrapolation is less reliable, given the cold bias of NCEP around Antarctica in JJA.

The difference is even larger for high levels. It seems that the NCEP reanalysis misses completely the maximum center (especially during Southern Hemisphere winter, JJA), with the value only half that of ECMWF. We can deduce that the growth of baroclinic instabilities should be very different in the two datasets (Simmons and Hoskins 1978).

Figure 6 plots the longitude-pressure diagrams of $\overline{v'T'}$ averaged over latitudes 40°S to 70°S. For the lower layers, the geographical positions are roughly the same in the two datasets, but values of NCEP are smaller than those of ECMWF. At the level of 200 hPa, we can distinguish four active centers from ECMWF dataset for both seasons. They are respectively over

Atlantic, Indian Ocean, Pacific and South America. The latter is weak in DJF and strong in JJA. For the other three centers, DJF intensity is slightly stronger than that of JJA. We can observe, by comparison, that these high-layer strong $\overline{v'T'}$ centers are very weak in NCEP. This discrepancy is probablly related to the difference in models' resolution and dissipation, since there are only few observations in this zone and the data are mainly model produced. Straus and Yang (1997) compared NCEP against NASA/DAO for the Northern Hemisphere winter, they found a similar situation as revealed by Fig. 6, but the value of NCEP is stronger and that of NASA/DAO is weaker.

3.4 Occurrence frequency and amplitude of transient events

Until now, our calculation was on the integrated quantities, and it does not give information on the individual events : their occurrence frequency and amplitude. To study the occurrence frequency, we can perform a simple calculation of the day-to-day correlation coefficient between NCEP and ECMWF for the whole period and for every geographical location.

The calculation has been performed for different variables characterizing the transient properties of the atmospheric circulation : v', u', T', $v'u'$, $v'T'$ and K_e. Since the obtained results are very similar among the variables, we show only the correlation map for the 200-hPa transient kinetic energy in Fig. 7 for the whole period of 1979 to 1993. In the equatorial strip, the correlation between NCEP and ECMWF is very small since the transient circulation is weak in the tropics. In the Northern Hemisphere, the correlation coefficient reaches more than 0.95, which confirms the good agreement between the two datasets. At the mid-latitudes of the Southern Hemisphere, the correlation coefficient can also reach 0.95 for the data-rich regions and 0.9 for the data-poor regions.

Figure 7 is obtained without removing the seasonal cycle that may enhance the correlation coefficient. To evaluate the influence of the seasonal cycle, a year-to-year permutaion procedure is used. For every geographical location, we calculate a lagged correlation coefficient by delaying one of the two time series by a lag of 1, 2, ..., 8 years respectively. In this manner, we construct a statistical ensemble and perform a t-test. It reveals that Fig.7 is statistically significant at 100% confidence level for the whole globe.

We can deduce from these results that the occurrence frequency and temporal evolution of transient events agree well between NCEP and ECMWF in the Southern Hemisphere. We can also deduce that the differences mentioned in the previous subsection are due to amplitude difference between NCEP and ECMWF.

In a similar way as for calculating the correlation map, we can also compute the space pattern correlation between the two datasets on the daily base. We use the mid-latitudes of both the Hemispheres (30°S-70°S and 30°N-70°N) where the transient activities are strong. Figure 8 displays the correlation coefficient and RMS difference for 200-hPa v' (other quantities have similar features and are not presented here). We can see that the agreement between ECMWF and NCEP is systematically better in the Northern Hemisphere than in the Southern Hemisphere since the correlation coefficient is larger and the RMS difference smaller.

From Fig. 8 we can also observe a temporal evolution of the agreement between ECMWF and NCEP. For the Northern Hemisphere, the agreement is good and stable for the whole period although a small tendency of improvement is present. A visible seasonal cycle can be identified in both Figs. 8a and 8b with degraded agreement in summer season. For the Southern Hemisphere, the seasonal cycle is less important. The tendency of improvement is large. Before

1989, we can observe large dispersion with bad correlation coefficients in many cases. The agreement between ECMWF and NCEP is particularly low for 1980 with a small correlation coefficient (less than 0.8) reached in March. From 1989 to the end, good agreement is obtained and the dispersion is also reduced for both space-pattern correlation and RMS difference. This feature is probably related to the fact that the observation network has been considerably improved in the recent years.

4 Conclusions

We have compared the reanalyses issued respectively by ECMWF and NCEP. Generally speaking, the mean fields are quite similar in the two datasets, although some systematic differences can be noticed. The temperature in ECMWF is 2.5°C colder than in NCEP at the equatorial tropopause. However the ECMWF's tropical troposphere is warmer than that of NCEP. Over Antarctica, NCEP is very cold in winter. This makes the sea-level pressure, extrapolated by using surface pressure and ambient air temperature, excessively high for Antarctica in winter (not shown here).

For the transient kinetic energy, meridional transient fluxes of angular momentum and sensible heat, the two datasets agree with each other in the Northern Hemisphere. However over the data-poor regions of the Southern Hemisphere, the transient properties in NCEP are systematically smaller than those in ECMWF. The discrepancy is about 20%. For the term $\overline{v'T'}$, this discrepancy can reach 50% at high layers of the atmosphere during the Southern Hemisphere winter. By calculating the day-to-day correlation coefficient (space-pattern correlation or temporal correlation), we have demonstrated that these differences are mainly due to the smaller

amplitude of transient waves in NCEP. However their occurrence frequency and their temporal evolution show good agreement between the two datasets.

At this stage, we can not judge the relative quality of NCEP and ECMWF reanalyses, but we suggest that the ECMWF's results could be closer to reality since the spatial resolution of its data assimilation system is better and this permits it to resolve baroclinic instability in a more satisfactory way. Several recent studies based on atmospheric general circulation models, for example, Boyle (1993), Williamson et al. (1995), or Boer and Denis (1997), show clearly the dependence of baroclinic instability on the resolution of models.

Given the important differences between NCEP and ECMWF reanalyses in terms of atmospheric transient activities, it is interesting to utilize these data to investigate the behaviors of synoptic flow in the Southern Hemisphere, including intraseasonal oscillations (Berbery and Vera 1996 ; Nogués-Paegle and Mo 1997 ; Sinclair et al. 1997), and especially to document their differences. This will be reported in a future paper. For the next stage, we will also investigate the hydrological cycle of the two datasets, since the works presented by Wang and Paegle (1996), Mo and Higgins (1996) show clearly that the hydrological cycle is still more sensitive to the model's performance and the quality of data assimilation system.

Acknowledgement We wish to thank ECMWF and NCEP/NOAA for providing the two reanalysis datasets. They are available through the Climate Data Base Project of IPSL and LMD. The data processing facilities for ECMWF data are provided by IDRIS. This work is partly supported by the PNEDC (French National Program on Climate Dynamics) and the Environment Program of the European Commission.

References

Berbery EH, Vera CS (1996) Characteristics of the Southern Hemisphere winter storm track with filtered and unfiltered data. J Atmos Sci 53 : 468-481

Boer GJ, Denis B (1997) Numerical convergence of the dynamics of a GCM. Clim Dyn 13 : 359-374

Boyle JS (1993) Sensitivity of dynamical quantities to horizontal resolution for a climate simulation using ECMWF (cycle 33) model. J of Climate 6 : 796-815

Edmon HJ Jr, Hoskins BJ, McIntyre ME (1980) Eliassen-Palm cross sections for the troposphere. J Atmos Sci 37 : 2600-2616

Gibson R, Kallberg P, Uppala S (1996) The ECMWF re-analysis (ERA) project. ECMWF Newsletter 73 : 7-17.

Hoskins BJ, James IN, White GL (1983) The shape, propagation and mean-flow interaction of large-scale weather systems. J Atmos Sci 40 : 1595-1612

Kalnay E, Coauthors (1996) The NCEP/NCAR 40-year reanalysis project. Bull Amer Meteor Soc 77 : 437-471

Mo KC, Higgins RW (1996) Large-scale atmospheric moisture transport as evaluated in the NCEP/NCAR and the NASA/DAO reanalyses. J of Climate 9 : 1531-1545

Nogués-Paegle J, Mo KC (1997) Alternating wet and dry conditions over South America during summer. Mon Wea Rev 125 : 279-291

Peixoto J P, Oort AH (1992) Physics of Climate. Amer Inst Phys, 520 pp.

Simmons AJ, Hoskins BJ (1978) The life cycles of some nonlinear baroclinic waves. J Atmos Sci 35 : 414-432

Sinclair MR, Renwick JA, Kidson JW (1997) Low-frequency variability of Southern Hemisphere sea level pressure and weather system activity. Mon Wea Rev 125 : 2531-2543

Straus DM, Yang Q (1997) Vertical structure and dominant horizontal scales of baroclinic waves in the NASA DAO and NCEP reanalyses. Mon Wea Rev 125 : 3266-3278

Wang M, Paegle J (1996) Impact of analysis uncertainty upon regional atmospheric moisture flux. J Geophys Res 101 : 7291-7303

Williamson DL, Kiehl JT, Hack JJ (1995) Climate sensitivity of the NCAR community climate model (CCM2) to horizontal resolution. Clim Dyn 11 : 377-397

Figure Caption :

Fig. 1. Latitude-pressure diagram showing the annual-mean temperature difference (K) between ECMWF and NCEP. Contour interval is 0.5 but isoline 0 is omitted.

Fig. 2. Latitude-pressure diagrams of the zonally-averaged transient kinetic energy, K_e, for respectively NCEP (left panels, a and b) and ECMWF (right panels, c and d). Two seasons are shown : DJF (December-January-February) at top and JJA (June-July-August) at bottom. Unit is $m^2\ s^{-2}$. Contour interval is 20.

Fig. 3. (a) 200-hPa annual-mean transient kinetic energy K_e diagnosed from NCEP. (b) Difference between ECMWF and NCEP. (c) RMS (root-mean-square) difference between ECMWF and NCEP. RMS difference is calculated by $\sqrt{\frac{1}{N}\sum\left(x_i - y_i\right)^2}$, where x_i and y_i are the loading of two vectors (time series) of length N (5479 days).

Fig. 4. Latitude-pressure diagrams of the zonally-averaged transient flux of westerly angular momentum $\overline{v'u'}$ ($m^2\ s^{-2}$). Contour interval is 10. The panel's disposition is the same as in Fig. 2.

Fig. 5. The same as Fig. 4, but for the transient flux of sensible heat $\overline{v'T'}$ (K m s^{-1}). Contour interval is 2.

Fig. 6. Longitude-pressure diagrams showing the transient flux of sensible heat, $\overline{v'T'}$ (K m s^{-1}), averaged from 40°S to 70°S. Contour interval is 2.

Fig. 7. Correlation map between ECMWF and NCEP, calculated through day-to-day 200-hPa transient kinetic energy. Contour interval is 0.05.

Fig. 8. (a) Day-to-day time evolution of space-pattern correlation coefficient calculated for respectively 30°N-70°N and 30°S-70°S. (b) As in (a) but for the RMS difference. Unit is m s^{-1}.

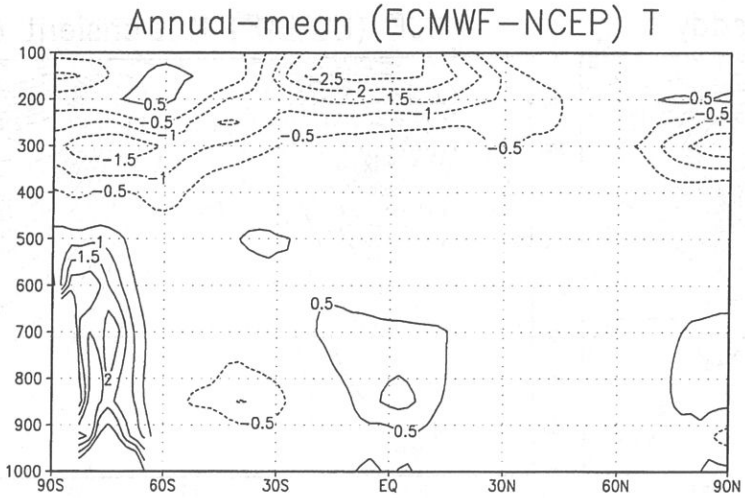
Annual−mean (ECMWF−NCEP) T
100
200
300
400
500
600
700
800
900
1000
90S
60S
30S
EQ
30N
60N
90N
0.5
−0.5
−1
−1.5
−2
−2.5
1
1.5
2

Figure 1

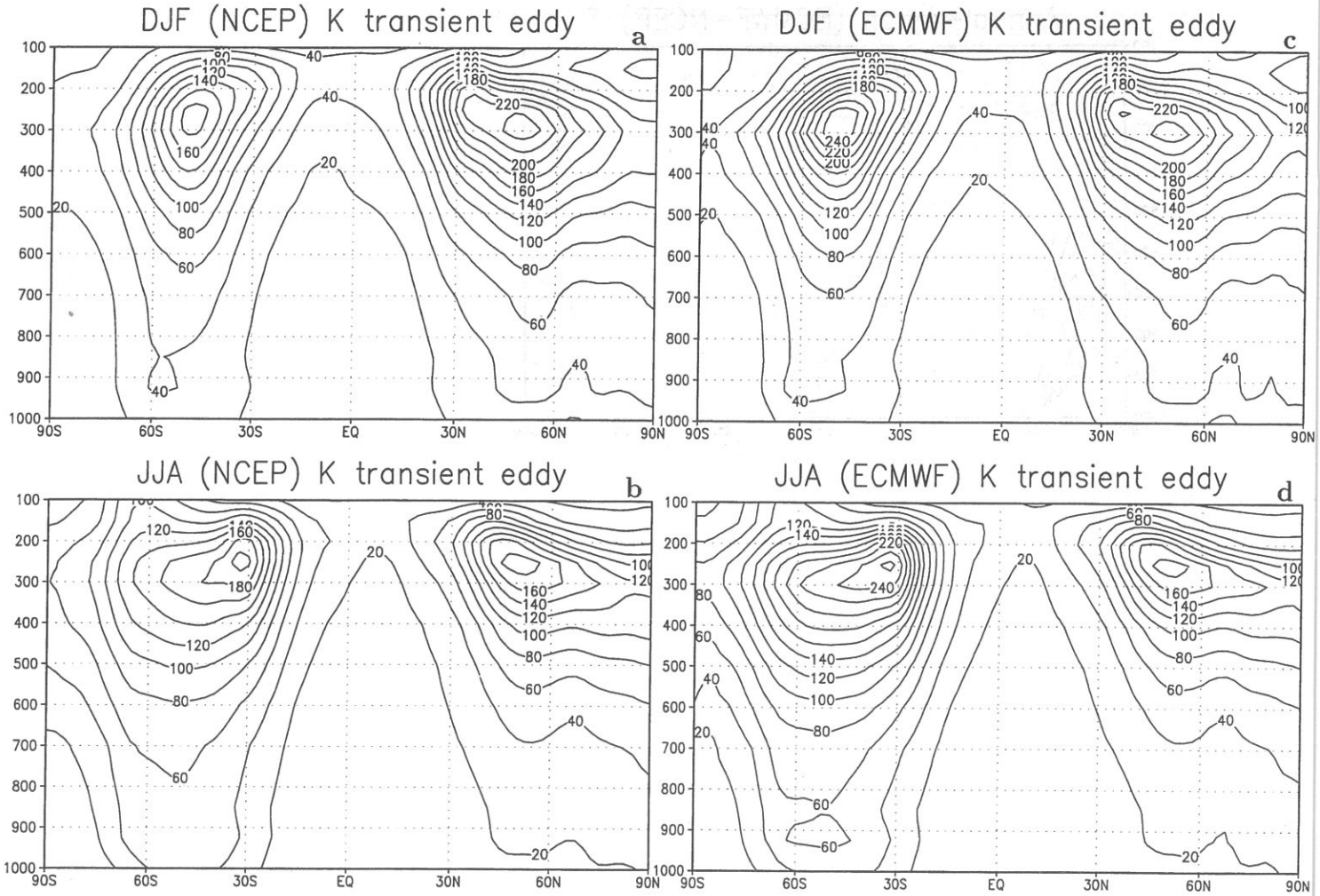
DJF (NCEP) K transient eddy
a
DJF (ECMWF) K transient eddy
c
JJA (NCEP) K transient eddy
b
JJA (ECMWF) K transient eddy
d
100
200
300
400
500
600
700
800
900
1000
90S
60S
30S
EQ
30N
60N
90N

Figure 2

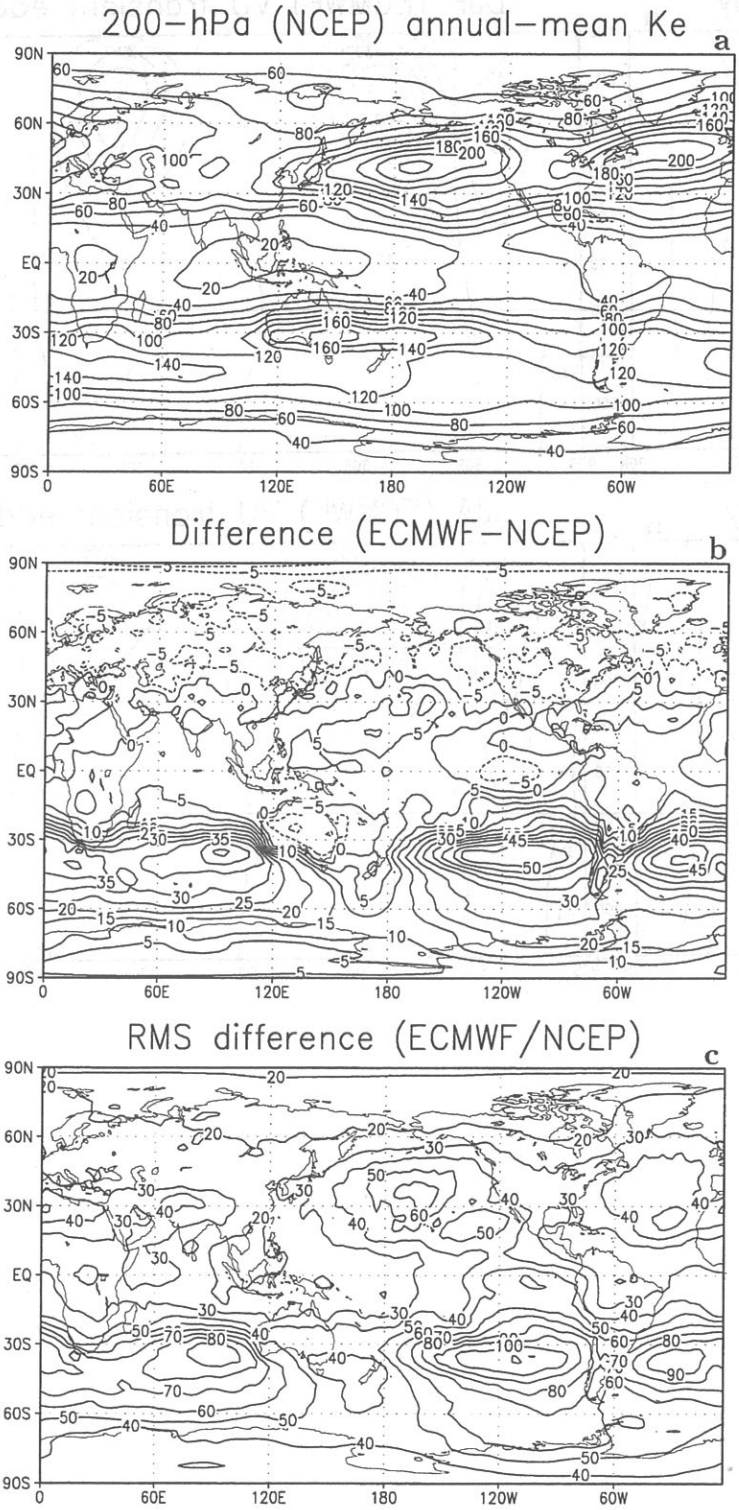
200-hPa (NCEP) annual-mean Ke
a
Difference (ECMWF-NCEP)
b
RMS difference (ECMWF/NCEP)
c
90N
60N
30N
EQ
30S
60S
90S
0
60E
120E
180
120W
60W

Figure 3

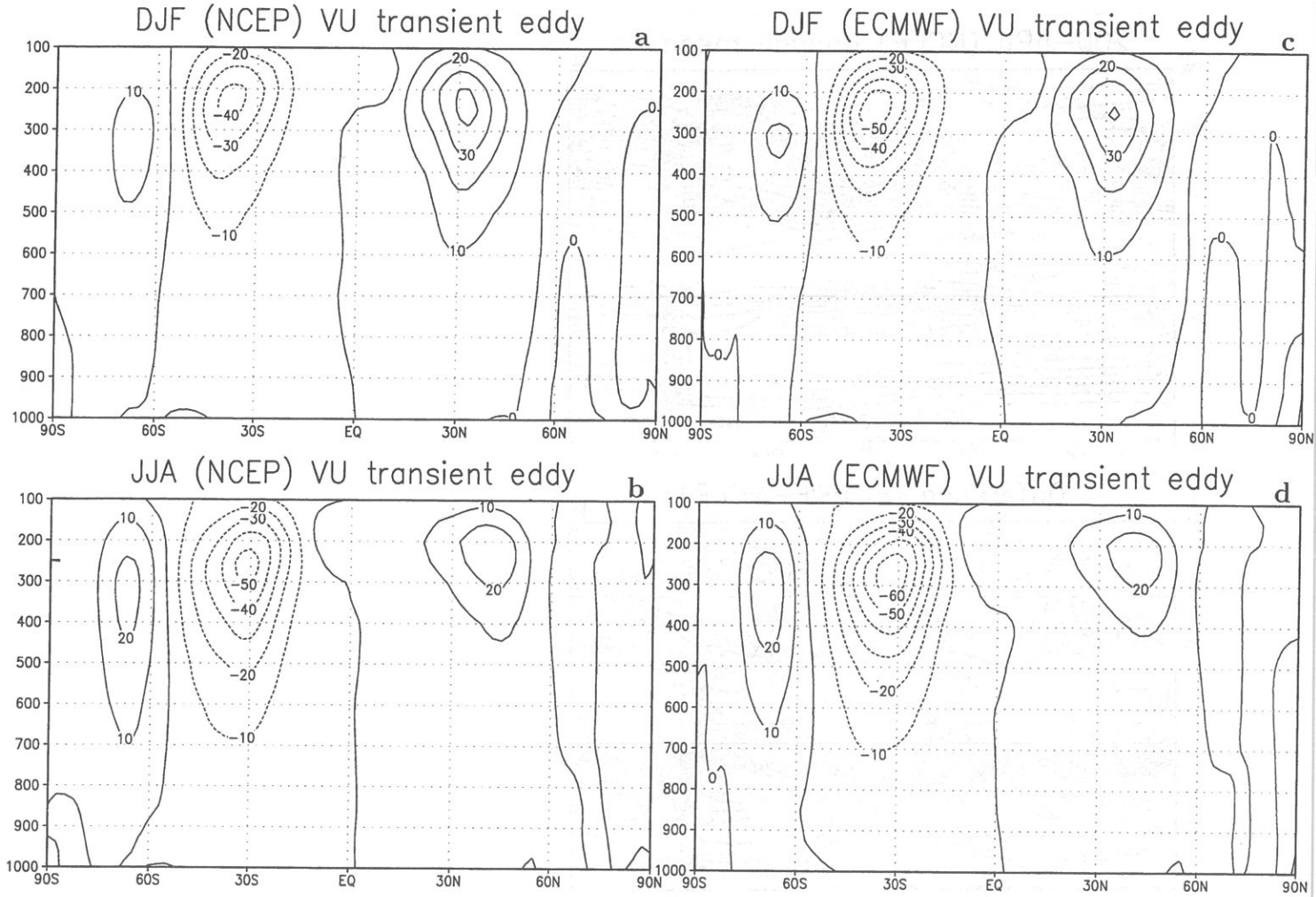
DJF (NCEP) VU transient eddy
a
DJF (ECMWF) VU transient eddy
c
JJA (NCEP) VU transient eddy
b
JJA (ECMWF) VU transient eddy
d
100
200
300
400
500
600
700
800
900
1000
90S
60S
30S
EQ
30N
60N
90N

Figure 4

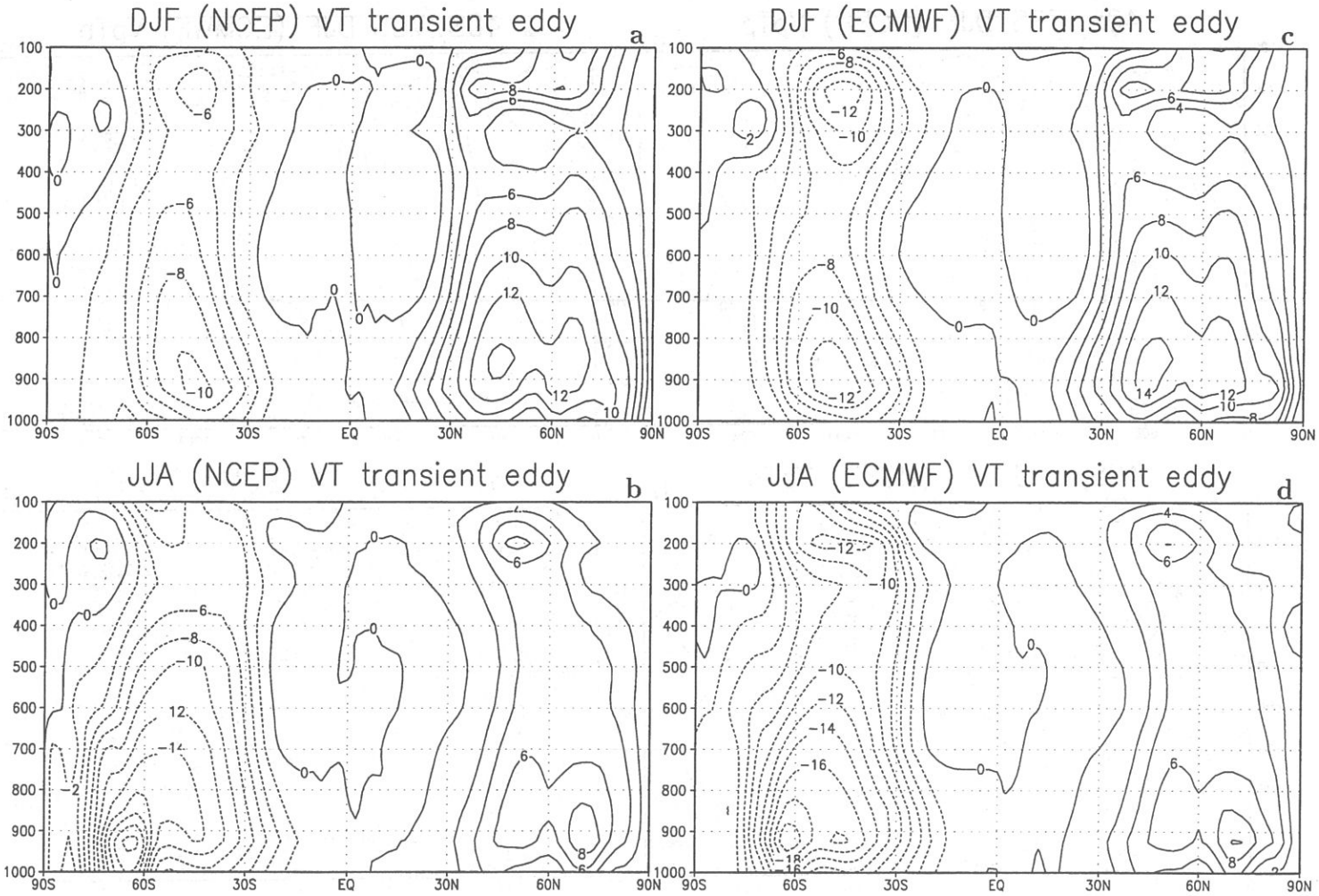
DJF (NCEP) VT transient eddy
a
DJF (ECMWF) VT transient eddy
c
JJA (NCEP) VT transient eddy
b
JJA (ECMWF) VT transient eddy
d
100
200
300
400
500
600
700
800
900
1000
90S
60S
30S
EQ
30N
60N
90N

Figure 5

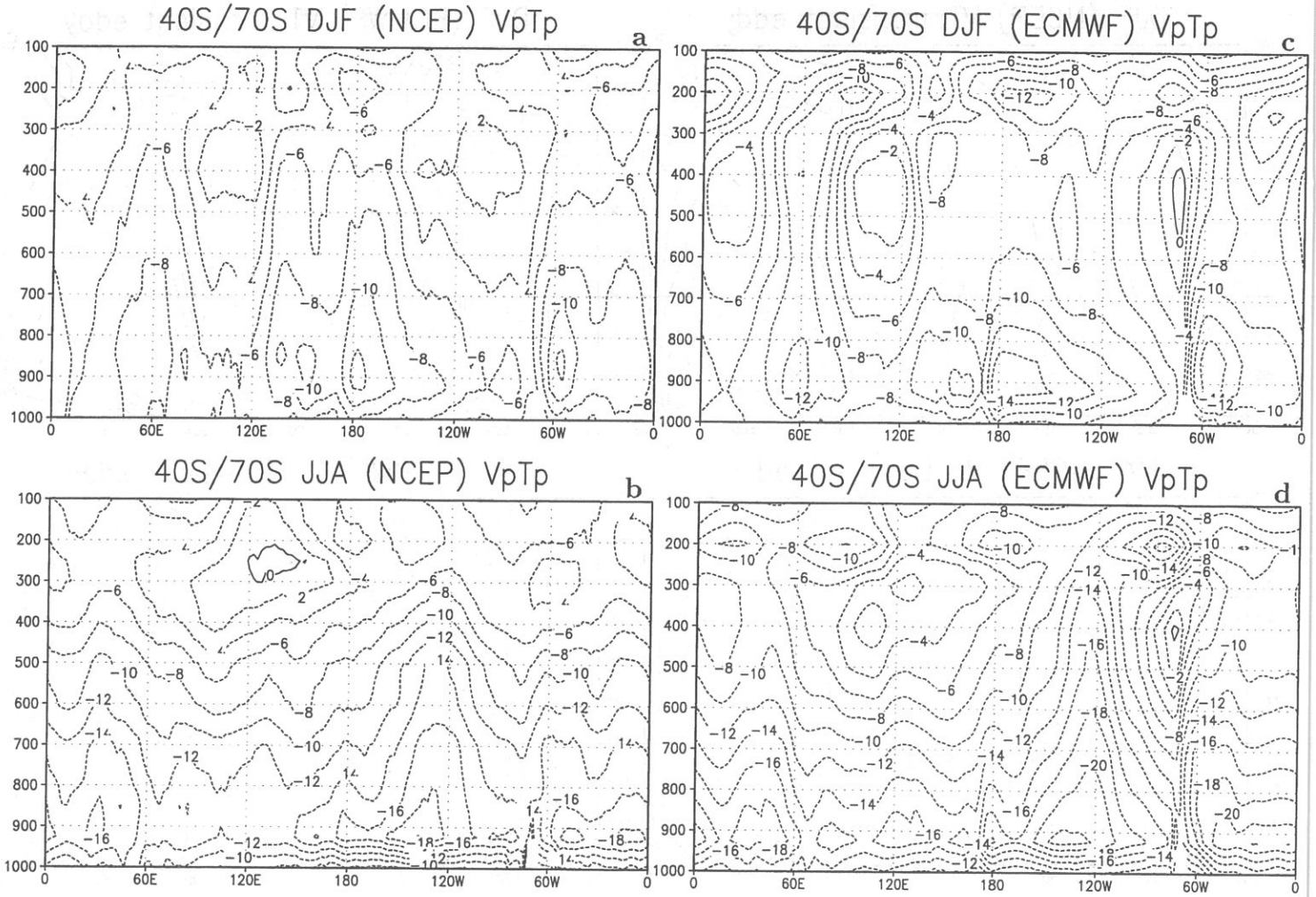
40S/70S DJF (NCEP) VpTp
a
40S/70S DJF (ECMWF) VpTp
c
40S/70S JJA (NCEP) VpTp
b
40S/70S JJA (ECMWF) VpTp
d
100
200
300
400
500
600
700
800
900
1000
0
60E
120E
180
120W
60W

Figure 6

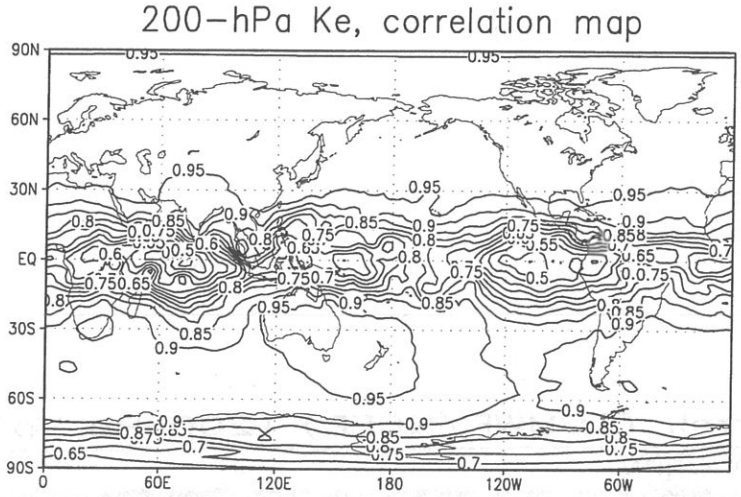
200−hPa Ke, correlation map
90N
60N
30N
EQ
30S
60S
90S
0
60E
120E
180
120W
60W

Figure 7

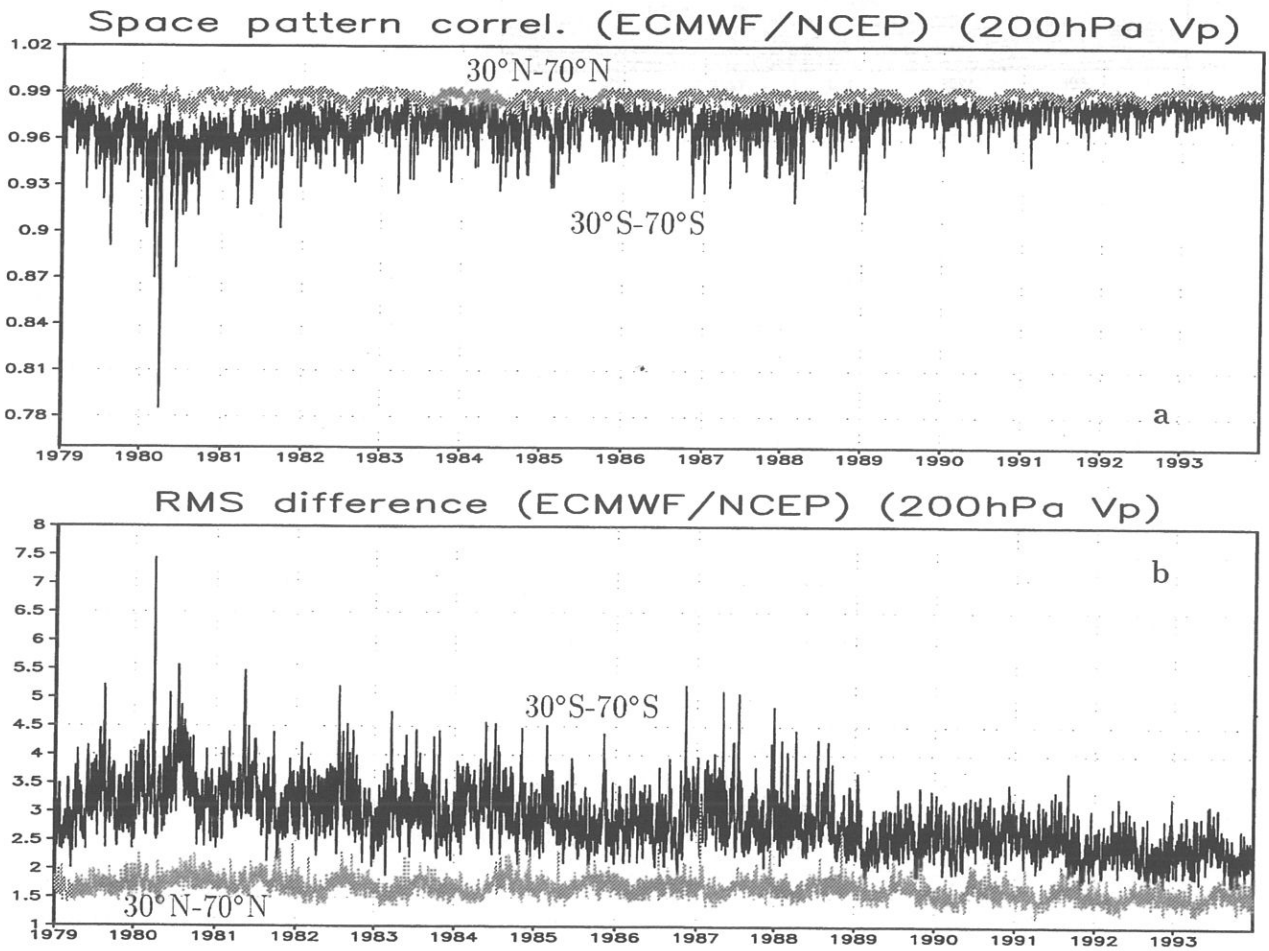
Space pattern correl. (ECMWF/NCEP) (200hPa Vp)
30°N-70°N
30°S-70°S
a
RMS difference (ECMWF/NCEP) (200hPa Vp)
b
30°S-70°S
30°N-70°N

Figure 8

Déjà paru :

1 : Janvier 1998 Agnès Ducharne, Katia Laval and Jan Polcher, *Sensitivity of the hydrological cycle to the parameterization of soil hydrology in a GCM*

2 : Janvier 1998 Marina Lévy, Laurent Mémery and Jean-Michel André , *Simulation of primary production and export fluxes in the Northwestern Mediterranean Sea*

3 : Février 1998 Valérie Masson, Sylvie Joussaume, Sophie Pinot and Gilles Ramstein, *Impact of parameterizations on simulated winter mid-Holocene and Last Glacial Maximum climatic changes in the Northern Hemisphere*

4 : Mars 1998 Jérôme Vialard et Pascale Delecluse, *An OGCM Study for the TOGA Decade. Part I: Role of Salinity in the Physics of the Western Pacific Fresh Pool, Part II: Barrier layer formation and variability*

5 : Avril 1998 O. Aumont, J. C. Orr, P. Monfray, and G. Madec, *Nutrient trapping in the equatorial Pacific: The ocean circulation solution*

6 : Mai 1998 Emmanuelle Cohen-Solal and Hervé Le Treut, *Long term climate drift of a coupled surface ocean-atmosphere model : role of ocean heat transport and cloud radiative feedbacks*

7 : Juin 1998 Marina Lévy, Laurent Mémery and Gurvan Madec, *Combined Effects of Mesoscale Processes and Atmospheric High-Frequency Variability on the Spring Bloom in the MEDOC Area*

8 : Septembre 1998 Carine Laurent, Hervé Le Treut, Zhao-Xin Li, Laurent Fairhead and Jean-Louis Dufresne, *The influence of resolution in simulating interannual and inter-decadal variability in a coupled ocean-atmosphere GCM, with emphasis over the North Atlantic.*

9 : Octobre 1998 Francis Codron, Augustin Vintzileos and Robert Sadourny, *An Improved Interpolation Scheme between an Atmospheric Model and Underlying Surface Grids near Orography and Ocean Boundaries.*

Plus de détails sont disponibles sur Internet :
http://www.ipsl.jussieu.fr/modelisation/liste-notes.html.